Additive Manufacturing Letters 2 (2022) 100028

Contents lists available at ScienceDirect

Additive Manufacturing Letters

journal homepage: www.elsevier.com/locate/addlet

Short Communication

Crack mitigation in laser engineered net shaping of WC-10wt%FeCr cemented carbides

Emma Molobi [a,b,*], Natasha Sacks [b,c], Maritha Theron [d]

[a] School of Chemical and Metallurgical Engineering, University of the Witwatersrand, Private Bag 3, Wits 2050, South Africa
[b] DSI-NRF Centre of Excellence in Strong Materials, South Africa
[c] Department of Industrial Engineering, Stellenbosch University, Private Bag X1, Matieland 7602, South Africa
[d] National Laser Centre, CSIR, Scientia 627-Jr, Meiring Naudé Road, Pretoria, South Africa

ARTICLE INFO

Keywords:
Directed energy deposition
Cracks
Cemented tungsten carbides
Thermal gradient

ABSTRACT

Laser engineered net shaping of a WC-10wt%FeCr cemented carbide showed cracking during deposition despite using a full factorial design of experiments matrix along with single and multiple objective optimization models to establish an optimal parameter set. In this study four techniques namely, laser re-melting, use of FeCr and Ni-alloy butter layers, and substrate preheating, were used in an effort to reduce the crack susceptibility of deposited samples and the resultant effects on microstructure and hardness were studied. Laser re-melting improved the surface morphology of the deposited samples and reduced the number of primary and secondary cracks, however the hardness decreased. The Ni-alloy butter layer reduced the formation of secondary cracking and led to an increase in hardness, while the FeCr butter layer resulted in increased primary cracks and a reduced hardness. Substrate preheating reduced crack formation and led to an increase in the hardness with the reduction in cracking being attributed to a reduction of the initial thermal gradient.

1. Introduction

Directed energy deposition (DED) is an additive manufacturing (AM) process with advantages such as fabrication of near net-shaped components, reduced usage of patterns and fixtures during fabrication, rapid manufacturing times and the production of materials with refined grains due to fast cooling rates [1,2]. The DED of cemented carbides offers an alternative manufacturing method to the conventional powder metallurgy (PM) production route which includes sintering as a process step [3,4]. The disadvantages of conventional sintering processes include long production times [5], grain growth due to long sintering times and solution re-precipitation of tungsten carbide (WC) crystals [6] and the formation of embrittling constituents such as the eta (η) phase due to decarburization [7].

DED may become a solution in the production of cemented carbides. However, the high cooling rates associated with laser fabrication processes due to a coherent high energy intensity being focused on small spot sizes [8], leads to residual stresses which may be problematic for cemented carbides. These stresses occur during non-uniform heating or cooling of a material leading to thermal contraction and expansion in response to the local thermal cycle [9]. During the cooling cycle in laser fabrication, shrinkage of the deposited material occurs due to thermal contraction. However, the heat is conducted into the substrate which causes it to expand and consequently contract as heat dissipates out of the material by convection [10]. When this expansion exceeds the contraction of a material, tensile residual stresses exist and if these exceed the yield strength of the material distortion and eventually cracking of the material will occur [11,12]. An additional source of residual stress is due to non-uniform expansion and contraction of materials during the thermal cycle which is governed by the differences in the coefficients of thermal expansion (CTE)/contraction between the substrate and the deposited material [13]. This may thus result in cracks at the interface [14].

WC, which is the main reinforcement material in cemented carbides, is known to be brittle due to its high hardness and hence has a high cracking susceptibility. Furthermore the use of iron (Fe) binders in cemented carbides display low rupture strength in comparison to other binders such as nickel (Ni) and cobalt (Co) [15]. Therefore, when WC and Fe are blended to produce a cemented carbide using DED then crack susceptibility is a concern due to the residual stresses mentioned earlier, and methods to mitigate crack formation need to be found. While research in crack restraining methods for cemented carbides fabricated by other laser manufacturing technologies such as laser cladding has been done by several researchers [16,17,18], similar research for DED fabrication of cemented carbides does not appear to have been published yet. Therefore, the focus of the current study was to investigate if the cracks from DED could be mitigated.

For laser cladding, substrate preheating is the most popular and studied crack restraining method. This involves preheating the

* Corresponding author.
E-mail address: Emma.Molobi@transnet.net (E. Molobi).

https://doi.org/10.1016/j.addlet.2022.100028
Received 9 November 2021; Received in revised form 28 December 2021; Accepted 8 January 2022

substrate to an optimized temperature in order to reduce the thermal gradient which occurs at high deposition temperatures, thereby reducing the residual stresses [14]. Buttering (also known as a buffer layer) is another method which has been used in the cladding and hard-facing industry in the field of dissimilar materials. The difference in the thermal coefficient of expansion and thermal stresses between the coating and the substrate may result in the formation of cracks as both materials don't contract at the same rate [14,19,20]. The butter layer is deposited at the interface between the substrate and the material alloy to be deposited, the function of the butter layer is to absorb the residual stresses [21]. It becomes clear that the butter layer should be composed of a material with a yield strength lower than that of the substrate and the alloy to be deposited. In addition the butter layer material should have a thermal coefficient of expansion which is between that of the substrate and alloy to be deposited [22].

Dai et al. [17], studied the effects of laser re-melting, annealing and preheating on the cracking susceptibility, microstructure and mechanical properties of WC/Fe laser cladding coatings. Laser re-melting was seen to reduce cracks on the surface, in addition laser re-melting gave rise to a smooth coating. During laser re-melting the temperature of the laser coating is higher than the laser cladding process, this thus results in lower cooling rates thus reducing the thermal stress which lowers the crack susceptibility [17]. Preheating which also lowers the cooling rate was seen to reduce the number of cracks on the coating. Dai et al. [17], showed that even though laser re-melting and preheating reduced the amount of cracks, these methods could not completely retrain the cracks. Luenda et al. [18] studied the application of preheating and the usage of a nickel-chromium (NiCr) buffer layer between the substrate and WC reinforced (NiCr) alloy coating. A maximum preheat temperature of 350 °C was not enough to ensure the deposition of crack-free samples and the use of a NiCr butter layer had no influence on the crack formation. Substrate preheating in order to reduce the cooling rate and hence prevent cracking, has been seen to reduce the crack propensity but not avoid cracking in cemented carbides with NiCr binders [16]. Sadhu et al. [23], established that optimizing the cooling rate by varying the scan speed in the direct metal laser deposition of NiCrSiBC-60%WC ceramic coating had no influence on the thermal crack formation. Preheating was seen to lower the thermal gradient and hence thermal residual stresses between the substrate and the coating resulting in a crack-free deposition [23].

According to the authors knowledge crack restraining methods have never been applied to directed energy deposited WC-FeCr cemented carbides. Thus three different crack restraining methods namely preheating, buttering and laser re-melting were investigated and the influence of these crack restraining methods on sample surface morphology, crack formation, phase formation and sample hardness was studied.

2. Materials and methods

2.1. Feedstock powders

Two feedstock powders namely, spherical cast WC powder with a particle size of 90±45 μm produced by Zhuzhou Jiangwe Boda Hard-facing Materials Co., Ltd; and a gas atomized AISI 420 (FeCr) powder with a particle size of 125±53 μm produced by Sandvik Osprey Ltd were used [24]. The powder morphology, particle size distribution (PSD) and phases analysis was determined by means of a Camscan Maxim 2000 scanning electron microscope (SEM), a Malvern Mastersizer-S and a Bruker D2 x-ray diffraction (XRD) spectroscopy respectively. The two powders, with a weight ratio of WC:FeCr alloy equal to 9:1, were blended in a rotary mill for 4 hrs at a rotation speed of 68.75 rpm [24].

2.2. LENS® deposition process

An Optomec 850-R LENS® system with a 1 kW IPG fiber laser was used for the deposition of WC-10wt%FeCr rectangular blocks onto a shot blasted mild steel substrate. The blocks were composed of 15 layers with dimensions 11 mm x 16 mm. During deposition the powders were delivered into the path of the laser beam through powder delivery nozzles. The interaction of the laser beam and feedstock powder led to the formation of a molten pool which formed a solid deposit upon solidification. Following deposition of each layer the laser head moved up by a constant z-increment of 0.2 mm, while the substrate remained stationary. The near optimum process parameters for the deposition are presented in Table 1. The near optimum process parameters were obtained from a full factorial design of experiments (DOE), establishment from statistical regression models and multi-objective optimization techniques in preliminary studies.

Table 1
LENS® process parameters.

Process parameter	Value
Laser power (W)	200
Traverse speed (mm/s)	3.2
Powder feed rate (g/min)	12.2
Z-increment (mm)	0.2
Stand-off distance (mm)	8
Laser spot size (mm)	1.4

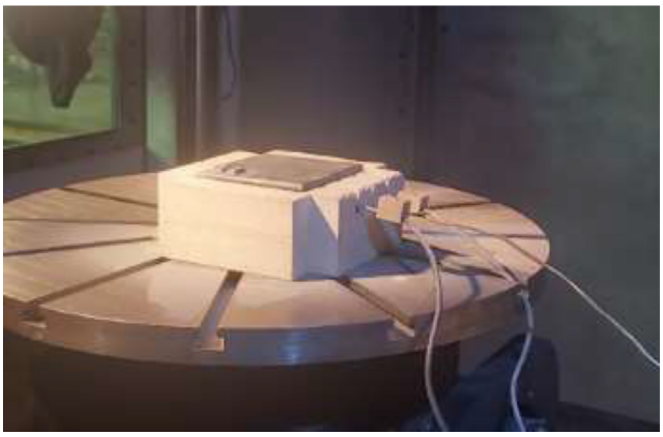

Fig. 1. Ceramic heating stage.

2.3. Crack restraining techniques

Experiments of the effects of different crack restraining methods, namely preheating, butter layer and laser re-melting were carried out. Preheating of the mild steel substrate before LENS® deposition was carried out by using a ceramic heating stage (Fig. 1), a preheat temperature of 250 °C [17], was used and verification was done using an infrared thermometer. During buttering two types of alloys were used, namely AISI 420 (FeCr) and Monel 400 butter (Ni-alloy). The butter layers were deposited using the process parameters shown in Table 1. A three layer butter was applied at the interface between the substrate and WC-10wt%FeCr deposit. Laser re-melting was carried out by depositing 15 layers of WC- 10wt%FeCr after which the powder nozzles were closed and the laser was used to heat the top surface of the deposited samples. In order to see the effects of laser re-melting, 1 and 3 layers of laser re-melting were conducted. The 3 layers laser re-melting technique was carried by heating the top surface 3 times (3 layer deposition) without the addition of powder.

2.4. Material characterization

The cross sections of the deposited samples were analysed for cracks using a liquid dye penetrant crack testing method. The cracks observed were visually counted and categorised into main and secondary cracks,

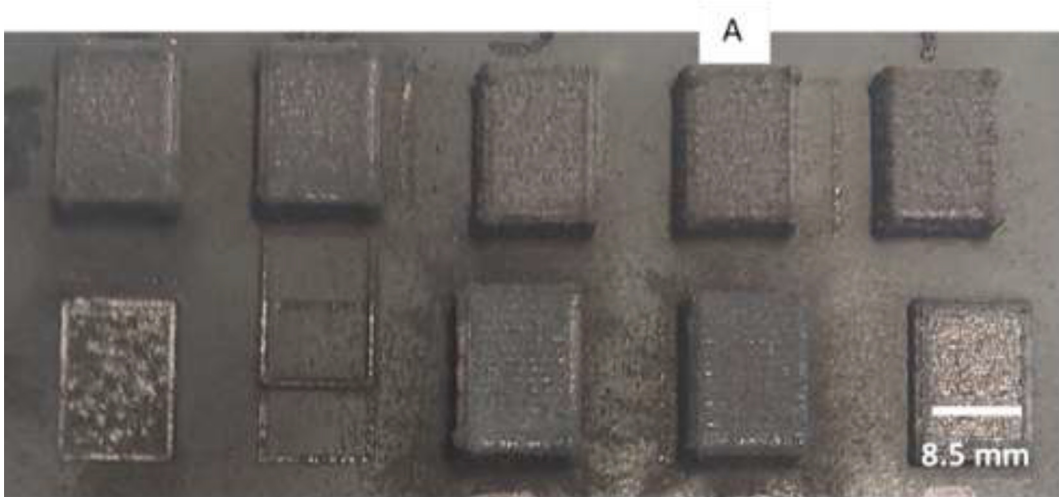

Fig. 2. Sample A, LENS deposited sample at 200 W, 3.2 mm/s, 12.2 g/min without crack mitigation.

whereby secondary cracks originated from the main cracks. In order to carry out metallographic and phase analysis the samples were hot mounted using Struers bakelite resin, ground using Struers diamond grinding discs grit 220 and 1200, respectively and polished with a 6 μm, 3 μm and 1 μm finish using a Struers diamond suspension. Un-etched samples were viewed using an Olympus stereo microscope. An Electron probe micro-analyzer (EPMA) was used to carry out elemental analysis around the crack area. Vickers macro-hardness measurements were done on the deposited cube samples using an Innovatest Nexus 8000 series universal hardness tester. A Vickers diamond indenter with a load of 30 kg load was used. Three indentations were randomly collected and averaged for each hardness value.

3. Results and discussion

3.1. Analysis of crack restraining methods

Fig. 2 shows the deposited WC-10wt%FeCr blocks before the application of crack restraining techniques. No cracks were visually visible on the surface of the deposited sample and this could have been due to the surface roughness of the sample.

Sample A was sectioned transversely and a dye penetrant test was conducted in order to identify the cracks on the cross section (Fig. 3). Vertical macro-cracks were seen to be propagating from the top surface transversely to the sample build direction until the substrate/deposit interface. Horizontal secondary cracks originating from the main cracks were also observed, evidence of secondary cracking shows that the material was under high internal stresses [25]. Toe cracks were also observed between the deposited sample and the substrate interface, these cracks are caused by excessive stress and a brittle heat affect zone (HAZ) [26], in addition the deposition toe (sample/substrate interface corner) causes a geometric stress raiser. The presence of cracks shows that the direct deposition of WC-10wt%FeCr results in high tensile stresses which exceeds the yield stress of the material. The material thus relieves these stresses by the formation of cracks.

3.1.1. Effect of laser re-melting on crack formation

Fig. 4 shows the surface morphology of the deposited samples before and after 1 and 3 layers of laser re-melting. Laser re-melting resulted in an improved surface appearance which visually appeared smoother with reduced edges on the contours and with less visibility of the scanning pattern than the samples without laser re-melting. During laser re-melting the top layers of the sample are heated and melted without the addition of powder, this then leads to the melting of the initial un-melted powder particles on the surface and re-melted material flow from peaks to valleys under surface tension [17,27,28].

Table 2
Influence of crack restraining methods on cracks.

Samples deposited at 200 W, 3.2 mm/s, 12.2 g/min	Nr. of main cracks
As deposited	4
FeCr (AISI 420) butter	5
Monel 400 (Ni alloy) butter	4
1 layer laser re-melting	4
3 layer laser re-melting	3
Preheating the substrate to 250 °C	3

No cracks were visually observed on the surfaces due to the surface roughness of deposited samples, however the cross sections displayed cracks which were perpendicular to the deposit-substrate interface, a reduction of secondary cracks was observed (Fig. 5). The 1 layer re-melting showed lack of fusion cracks along the interface, however this was due to material pull-out during metallographic preparation. Not only is laser re-melting used to improve the surface quality of laser deposited samples but it can also be used as an in-situ post heat treatment process to retard crack growth and reduce cracks [29,30]. One layer laser re-melting had no influence on the cracks as the number of cracks were the same with samples without laser re-melting. However a 3-layer laser re-melting resulted in a 25% reduction in the number of cracks (Table 2). Laser re-melting increases the overall temperature of the fabricated WC-10wt%FeCr sample with the top layers experiencing the highest temperature, this increase in temperature results in slower cooling rates and a reduction in the thermal gradient thus decreasing the thermal residual stresses [23].

3.1.2. Effect of FeCr butter layer on crack formation

An FeCr butter layer was used to attain compatibility with the binder phase of the deposited samples and to ensure that the coefficient of thermal expansion was similar to that of the deposited material. A WC-FeCr cemented carbides, FeCr alloy and mild steel material have CTE's of 7×10^{-6} °C^{-1} [31], 10.25×10^{-6} °C^{-1} and 11.7×10^{-6} °C^{-1} [32], respectively. A butter layer having an intermediate CTE between the substrate and the deposited material reduces the thermal residual stresses and hence reduce susceptibility to crack formation [33]. Even though the FeCr butter layer had an intermediate CTE it was observed that there was an increase in the number of main cracks which were perpendicular to the substrate-butter layer interface, and a reduction in secondary cracks (Fig. 6). FeCr alloys namely AISI 420 are fracture sensitive and have

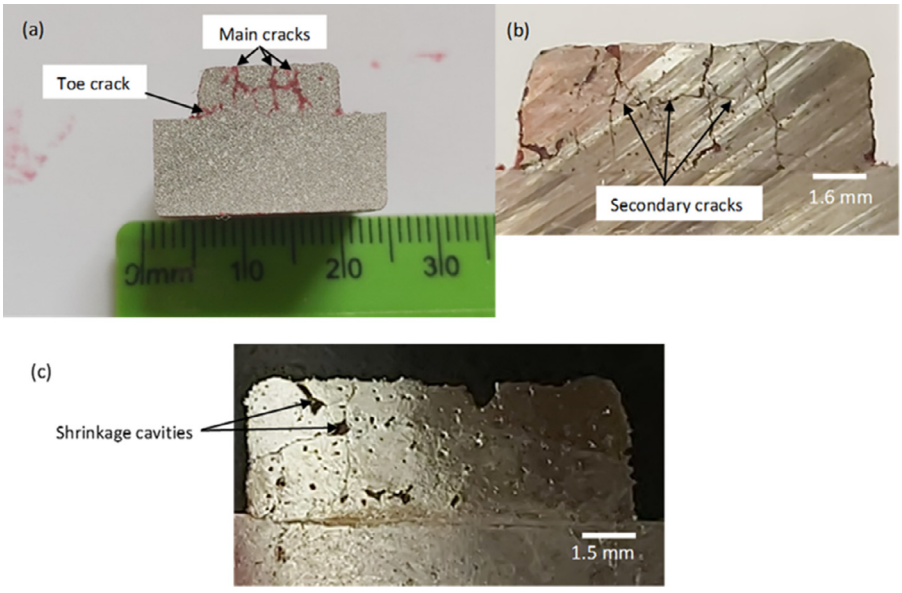

Fig. 3. Cracks on samples deposited at 200 W, 3.2 mm/s, 12.2 g/min; (a) Dye penetrant tested sample, (b) As-sectioned cross section, (c) As-polished cross section.

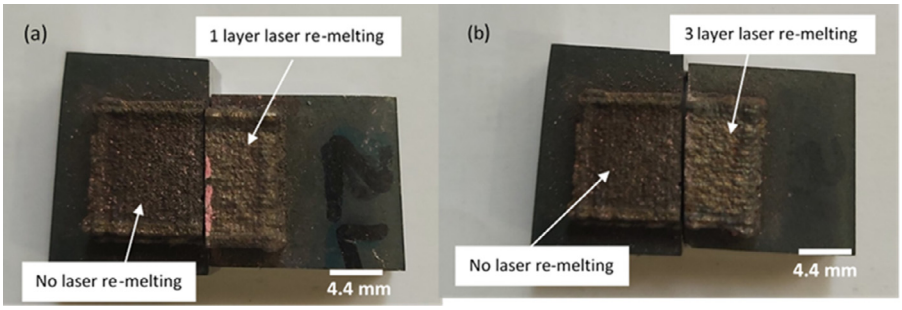

Fig. 4. Surface characteristics of; (a) 1 layer and (b) 3 layer laser re-melting.

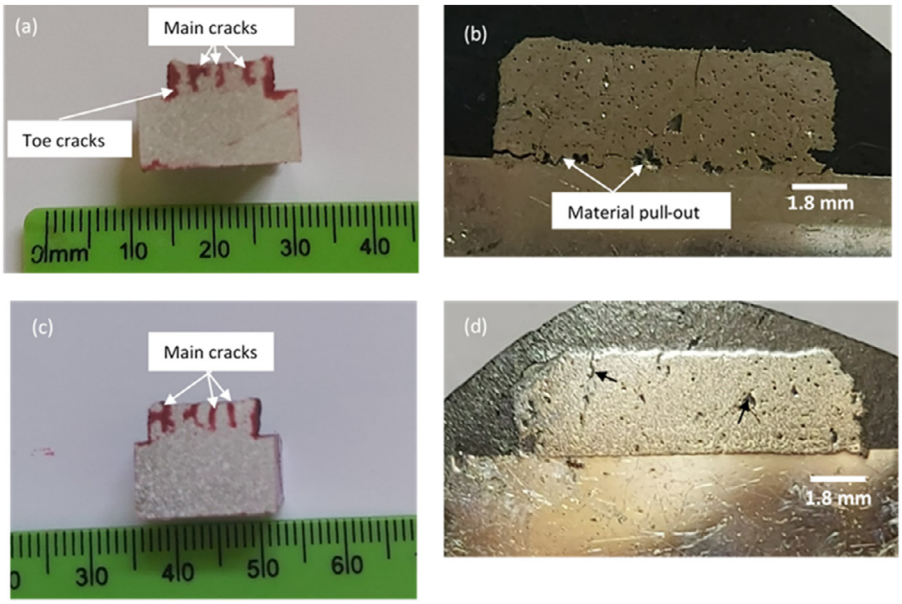

Fig. 5. Effect of laser re-melting, (a) and (b) 1 layer re-melting; (c) and (d) 3 layers re-melting.

microstructures composed of brittle martensite and retained austenite following laser deposition [34].

3.1.3. Effect of Ni-alloy butter layer on crack formation

The use of Ni-alloys as butter layers have been extensively used in order to reduce the thermal residual stresses by applying a bond coat material. The bond coat material has a coefficient of thermal expansion intermediate between the substrate and the material to be deposited [20,18]. Leunda et al. [18], however discovered that the use of a NiCr butter layer was not sufficient in avoiding cracks in cemented carbides. In this study a Monel 400 butter layer having a coefficient of thermal expansion of 14.5×10^{-6} °C^{-1} exceeding that of the substrate and the

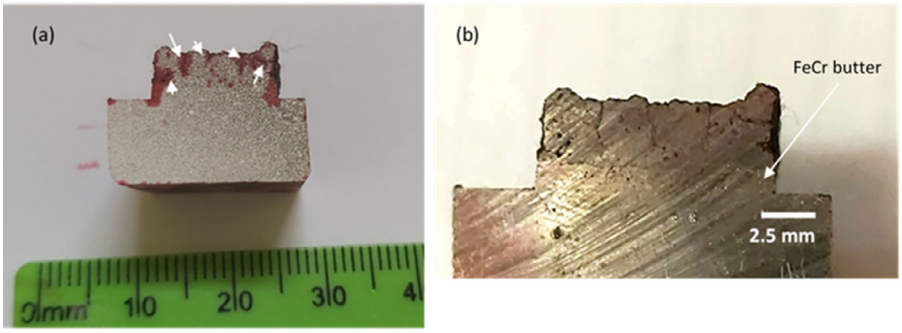

Fig. 6. FeCr butter layer; (a) dye penetrant image, (b) macro-image showing cracks.

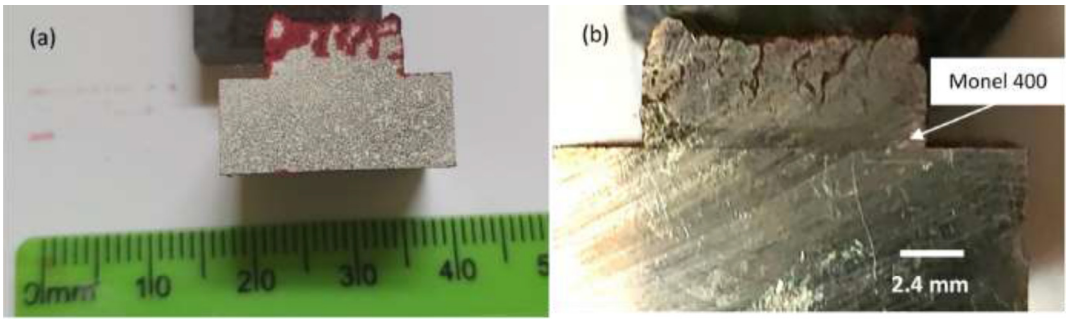

Fig. 7. Ni-alloy butter; (a) dye penetrant sample, (b) macro-image showing cracks.

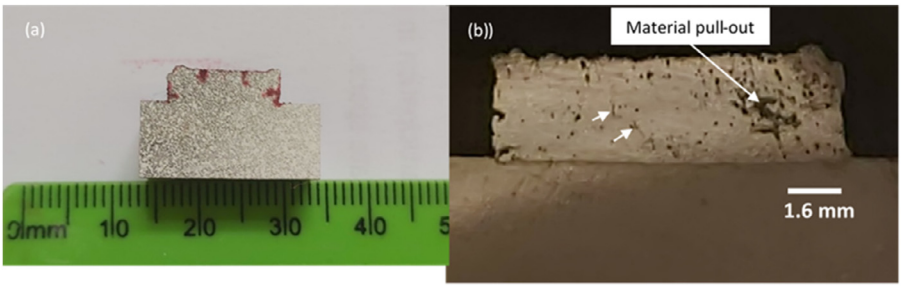

Fig. 8. Preheat at 250 °C; (a) dye penetrant sample, (b) macro-image.

WC-FeCr cemented carbide was used. The reason of usage is because Monel 400 has a yield strength of 240 MPa [35] and its lower than that of AISI 420 (FeCr) which is 532 MPa [36], which means Monel 400 will be able to absorb the plastic strain during deposition. In addition Monel 400 has a lower thermal conductivity than mild steel hence a slower cooling rate will be imparted by the butter layer. Following deposition using the Ni-alloy butter layer, cracks were still observed on the sample cross section (Fig. 7). The butter layer had no influence on the internal cracks as the same number of cracks were present with or without the Ni-alloy butter layer, however there was a reduction in the formation of secondary cracking.

3.1.4. *Effect of substrate preheat on crack formation*

The mild steel substrate was preheated to 250 °C after which the WC-10wt%FeCr powder was deposited onto the preheated substrate. Cracks were observed even after preheating (Fig. 8). The preheated sample however, had a reduced number of cracks in comparison to the samples which did not undergo preheat (Table 2) and no secondary cracking was observed.

3.2. *Effect of crack restraining methods on microstructure*

The cracks present on the WC-FeCr were seen to propagate through the spherical WC grains and FeCr matrix (Fig. 9). EPMA analysis was conducted and it was established that elemental segregation of carbon was present along the crack path (Fig. 10). It becomes clear that cracking initiates and propagates along stress raisers such as carbon precipitates, design notches and brittle WC grains.

Fig. 11, shows the XRD spectrums of the phases present in all the crack restraining samples and these were compared with the sample without any crack restraining methods. The use of a Ni-alloy butter layer led to NiCu peaks with no secondary chromium carbide formation and the FeCr butter layer led to the formation of stronger Cr_7C_3 peaks. The presence of $Cr7C_3$ causes a material to be brittle and thus reduces the fracture toughness [37]. It is clear that the use of the butter layer and substrate preheating results in the introduction of additional phases.

3.3. *Effect of crack restraining methods on hardness*

Fig. 12 shows that laser re-melting and the application of the FeCr butter layer resulted in a decrease in hardness of the WC-10wt%FeCr cemented carbide. The 3 layer re-melting process was seen to have a major impact on hardness reduction than the 1 layer re-melting process. Laser re-melting results in increased WC dissolution leading to a reduction in hardness. This is in agreement to the results obtained by Dai et al. [17] and Leunda et al. [18]. The use of a Ni-alloy butter layer and a substrate preheat of 250 °C resulted in an increase in the sample hardness in comparison with samples deposited without the use of crack restraining techniques, with preheat displaying the highest hardness. Winarto et al. [20] and Nagentrau et al. [38]

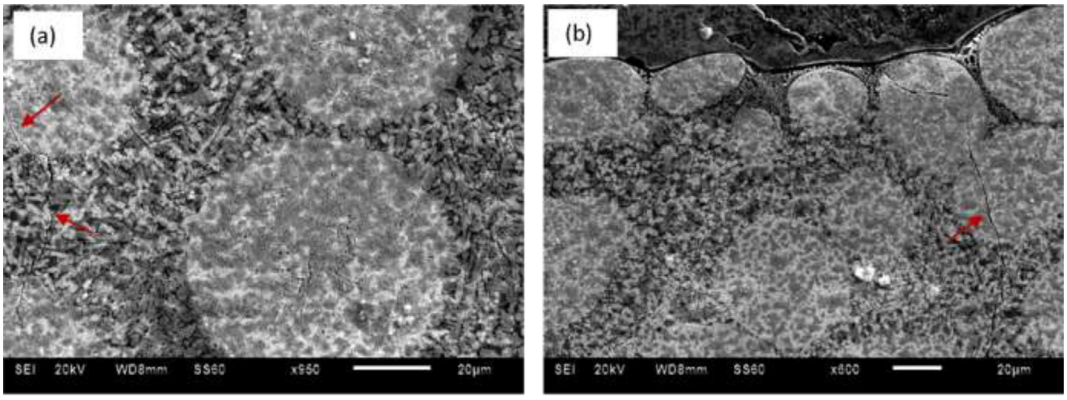

Fig. 9. Cracks on sample deposited without crack restraining; (a) center of sample, (b) substrate/deposit interface.

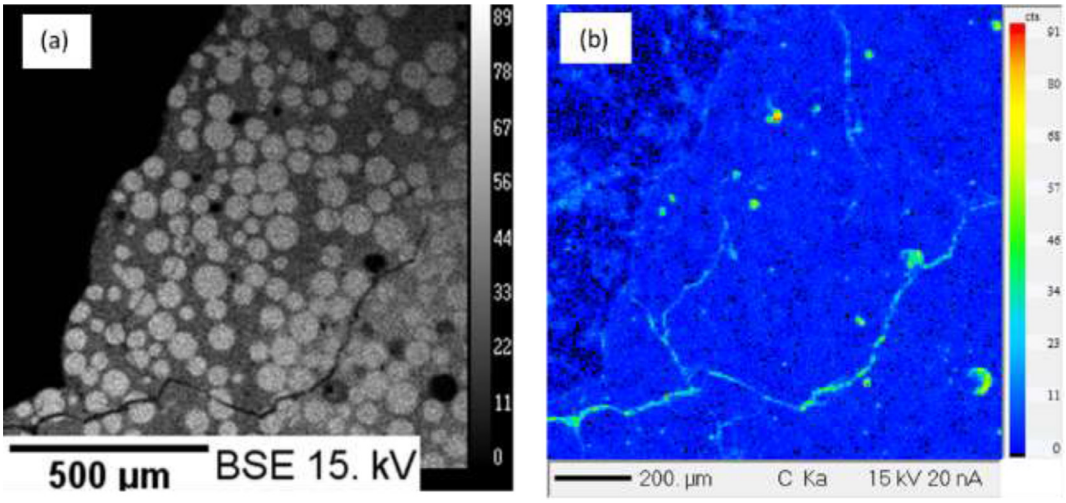

Fig. 10. (a) Micrograph of showing crack propagation; (b) EPMA analysis showing carbon segregation along the crack path.

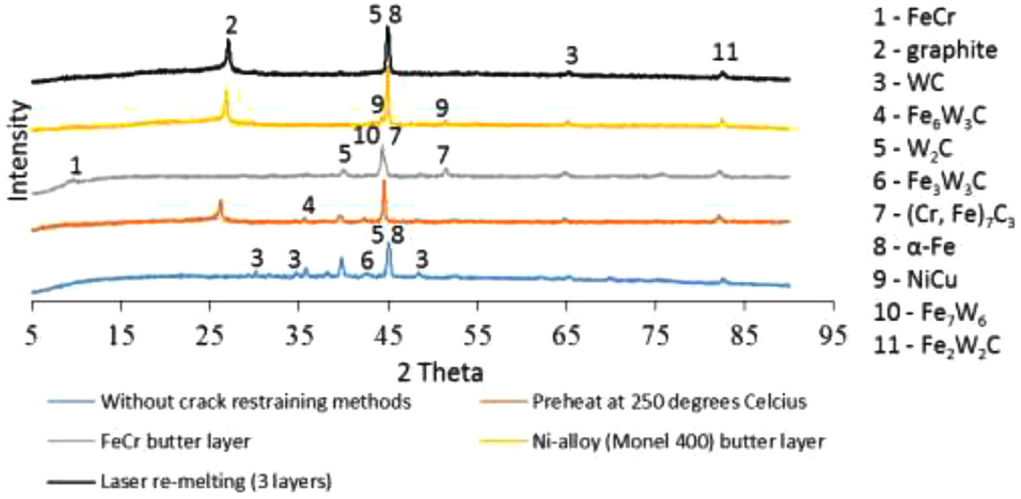

Fig. 11. XRD spectrum of the different crack restraining methods.

also indicated that hardness of Ni buttered coatings increased with the application of substrate preheat and this was attributed to the distribution of carbides within the coating. The use of the Ni-alloy butter layer resulted in an increase in hardness, this could be attributed to the dilution-limiting effect of the iron based substrate material, preventing the diffusion of iron (Fe) and hence prevented the formation of chromium carbides. This is concurrent with the work done by Stanciu et al. [19], whereby the use of a Ni-alloy butter resulted in increased hardness.

4. Conclusion

In this study, four approaches namely laser re-melting, substrate preheating and the use of a FeCr and Ni-alloy butter layers were explored

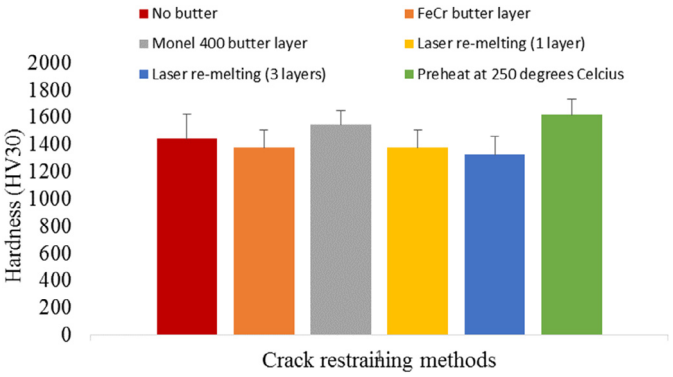

Fig. 12. Influence of the crack restraining methods on hardness.

to investigate their effect on crack restraining in the LENS® deposition of WC-10wt%FeCr cemented carbides. While none of the methods produced crack-free samples, all crack retraining methods led to a reduction in the secondary cracks. Laser re-melting, the use of a Ni-alloy and FeCr butter and substrate preheating led to a reduction in the amount of secondary cracks. However, laser re-melting and substrate preheating resulted in an overall decrease in the number of main cracks due to imparting slower cooling rates and hence a reduction in thermal residual stresses. The FeCr butter layer resulted in an increase in the number of cracks and this was attributed to the precipitation of chromium carbides such as $Cr7C_3$ on grain boundaries thus increasing the susceptibility to crack formation. The crack restraining techniques had an impact on the average hardness of the WC-10wt%FeCr with laser re-melting and the FeCr butter layer resulting in a decrease in the hardness. Laser re-melting resulted in an increase in temperature of the deposited sample leading to carbide dissolution and hence a decrease in hardness. The decrease in hardness when using a FeCr butter layer was attributed to carbide precipitation on grain boundaries thus increasing the susceptibility to crack formation. Localised distribution of carbides within the grain boundaries results in carbide depletion areas adjacent to the grain boundaries and hence reduction in hardness. The use of a Ni-alloy butter layer and substrate preheating lead to an increase in hardness.

Declaration of Competing Interest

None.

Acknowledgments

The authors wish to acknowledge the financial support received from the Department of Science and Innovation and the National Research Foundation in South Africa (Grant Nos.: 41292 and 129313). The National Laser center (NLC) at the Council for Scientific and Industrial Research (CSIR) is acknowledged for use of the LENS® machine as well as technical support (Grant No.: LREPA25).

References

[1] T.S. Srivatsan, T.S. Sudarshan (Eds.), Additive Manufacturing : Innovations, Advances, and Applications, CRC Press, 2015, doi:10.1201/B19360.
[2] Griffith, M.. et al. (2000) Understanding the microstructure and properties of components fabrication by laser engineered net shaping. Nashville. doi:10.1557/PROC-625-9.
[3] Y. Xiong, et al., 'Processing and microstructure of WC-CO cermets by laser engineered net shaping', in: Proceedings of the 19th Annual International Solid Freeform Fabrication Symposium, SFF 2008,, 2008, pp. 116–127, doi:10.26153/TSW/7256.
[4] J.A. Picas, et al., Microstructure and wear resistance of WC – Co by three consolidation processing techniques, Int. J. Refract. Met, Hard Mater. 27 (2009) 344–349, doi:10.1016/j.ijrmhm.2008.07.002.
[5] N. Joshi, U. Dixit, Lasers Based Manufacturing, Springer, 2014 Available at: https://www.springer.com/gp/book/9788132223511 .
[6] G. Gupta, et al., Processing and fabrication of advance materials XIII, in: Proceedings of the Conference Organized by National University of Singapore, Singapore Institute of Manufacturing Technology, Stallion Press (S) Pty.Ltd., Singapore, 2005, doi:10.1142/w001.
[7] G.S. Upadhyaya, Cemented Tungsten Carbides, Production, Properties and Testing, Noyes Publication, New Jersey, 1998.
[8] T. Kik, Heat source models in numerical simulations of laser welding, Materials 13 (2020) 1–24, doi:10.3390/ma13112653.
[9] M. Arunkumar, et al., Effect of plasma arc welding on residual stress and distortion of thin titanium sheet, Mater. Res. 22 (6) (2019), doi:10.1590/1980-5373-mr-2019-0366.
[10] J. Dowden, W. Schulz (Eds.), The Theory of Laser Materials Processing - Heat and Mass Transfer in Modern Technology, Springer, Switzerland, 2017 Available at: https://www.springer.com/gp/book/9789400789593 .
[11] L. Zhao, et al., Comparison of residual stresses obtained by the crack compliance method for parts produced by different metal additive manufacturing techniques and after friction stir processing, Addit. Manuf. 36 (5) (2020) 1–32, doi:10.1016/j.addma.2020.101499.
[12] R. Acevedo, et al., Residual stress analysis of additive manufacturing of metallic parts using ultrasonic waves: state of the art review, J. Mater. Res. Technol. 9 (4) (2020) 9457–9477, doi:10.1016/J.JMRT.2020.05.092.
[13] P. Farahmand, R. Kovacevic, Laser cladding assisted with an induction heater (LCAIH) of Ni–60%WC coating, J. Mater. Proc. Technol. 222 (2015) 244–258, doi:10.1016/J.JMATPROTEC.2015.02.026.
[14] O'Brien, A. (2011) 'Welding Handbook, Volume 4 - Materials and Applications, Part 1 (9th Edition)', Welding Handbook, Volume 4 - Materials and Applications, Part 1 (9th Edition), 1. Available at: https://app.knovel.com/hotlink/toc/id:kpWHVMAP01/welding-handbook-volume/welding-handbook-volume (Accessed: 15 July 2021).
[15] Humenik, M., Moskowitz, D. and Park, A. (1967) 'Iron bonded tungsten carbide'. United States Patent US3384465A.
[16] J.M. Amado, et al., Crack free tungsten carbide reinforced Ni(Cr) layers obtained by laser cladding, Phys. Proced. 12 (PART 1) (2011) 338–344, doi:10.1016/J.PHPRO.2011.03.043.
[17] Q.L. Dai, F.Y. You, C. Luo, Crack restraining methods and their effects on the microstructures and properties of laser cladded WC/Fe Coatings, Materials 11 (2018) 1–13, doi:10.3390/ma11122541.
[18] J. Leunda, C. Soriano, C. Sanz, Inner walls laser cladding of WC reinforced Ni coatings, in: Proceedings of the Lasers in Manufacturing Conference, Eibar (Gipuzkoa), Spain, 2015.
[19] Stanciu, E.M. et al. (2016) 'Dual Coating Laser Cladding of NiCrBSi and Inconel 718', http://dx.doi.org/10.1080/10426914.2015.1103866, 31(12), pp. 1556–1564. doi: 10.1080/10426914.2015.1103866.
[20] W. Winarto, N. Sofyan, D Rooscote, Effect of bond coat and preheat on the microstructure, hardness, and porosity of flame sprayed tungsten carbide coatings, in: Proceedings of the AIP Conference, 2017, p. 1855, doi:10.1063/1.4985486.
[21] X.L. Shi, et al., Mechanical properties, phases and microstructure of ultrafine hardmetals prepared by WC-6.29Co nanocrystalline composite powder, Mater. Sci. Eng. A 392 (1–2) (2005) 335–339, doi:10.1016/J.MSEA.2004.09.043.
[22] C.C. Berndt, Thermal spray surface engineering via applied research, in: Proceedings of the 1st International Thermal Spray Conference, Montréal , Québec , Canada, ASM International, 2000, p. 1410.
[23] A. Sadhu, et al., A study on the influence of substrate pre-heating on mitigation of cracks in direct metal laser deposition of NiCrSiBC-60%WC ceramic coating on Inconel 718, Surf. Coat. Technol. 389 (2020) 1–14, doi:10.1016/J.SURFCOAT.2020.125646.
[24] E. Molobi, N. Sacks, M. Theron, Feasibility of using Laser Enabled Net Shaping to manufacture WC-Fe alloys, in: Proceedings of the Euro PM2018 (Powder Metallurgy) Congress and Exhibition, Bilboa, 2018, pp. 1–6.
[25] L.C.F. Canale, R.A. Mesquita, G.E. Totten, Failure Analysis of Heat Treated Steel Components, ASM International, Ohi, 2008 Available at: www.asminternational.org (Accessed: 3 August 2021).
[26] G. Kelkar, Weld Cracks - an engineer's worst nightmare, WMJ Technol. 562 (2014) 743–757.
[27] S. Marimuthu, et al., Laser polishing of selective laser melted components, Int. J. Mach. Tools Manuf. 95 (2015) 97–104, doi:10.1016/J.IJMACHTOOLS.2015.05.002.
[28] Y. Zhao, et al., Investigation on the effect of laser remelting for laser cladding nickel based alloy, J. Laser Appl. 31 (2) (2019) 022512, doi:10.2351/1.5096126.
[29] X. Zhao, H. Zhang, Y. Liu, Effect of laser surface remelting on the fatigue crack propagation rate of 40Cr steel, Results Phys. 12 (2019) 424–431, doi:10.1016/J.RINP.2018.11.097.
[30] S. Zhou, et al., Effect of laser remelting on microstructure and properties of WC reinforced Fe-based amorphous composite coatings by laser cladding, Opt. Laser. Technol. 103 (2018) 8–16, doi:10.1016/J.OPTLASTEC.2018.01.024.
[31] S.A. Humphry-Baker, et al., Thermophysical properties of Co-free WC-FeCr hardmetals, in: Proceedings of the 19th Plansee Seminar International Journal of Refractory Metals and Hard Materials, Oxfordshire, 2017.
[32] Laser and Optics User's Manual: Linear Thermal Expanison Coefficients of Metals and Alloys (2002). U.S.A.
[33] N. Thawari, et al., Influence of buffer layer on surface and tribomechanical properties of laser cladded Stellite 6, Mater. Sci. Eng. B Solid State Mater. Adv. Technol. 263 (2021) 1–9, doi:10.1016/J.MSEB.2020.114799.
[34] S. Da Sun, et al., In-situ quench and tempering for microstructure control and enhanced mechanical properties of laser cladded AISI 420 stainless steel powder on 300M steel substrates, Surf. Coat. Technol. 333 (2018) 210–219, doi:10.1016/J.SURFCOAT.2017.10.080.
[35] C. Mani, S. Balasubramani, R. Karthikeyan, Finite element simulation on effect of bevel angle and filler material on tensile strength of 316 L stainless steel/Monel

400 dissimilar metal welded joints, Mater. Today Proc. 28 (2019) 1048–1053, doi:10.1016/J.MATPR.2019.12.353.
[36] ASME Boiler and Pressue Vessel Code, Section II, Part D (2010).
[37] K. Hao, et al., Effect of heat input on weld microstructure and toughness of laser-arc hybrid welding of martensitic stainless steel, J. Mater. Proc. Technol. 245 (2017) 7–14, doi:10.1016/J.JMATPROTEC.2017.02.007.
[38] Nagentrau, M. et al. (2019) 'Preheat treatment on the tungsten carbide hardfacing: microstructure analysis', IOP Conference Series: Materials Science and Engineering, 505(1). doi: 10.1088/1757-899X/505/1/012150.